PHOTOELECTROCHEMICAL AND SOLAR CELL STUDIES OF n-CdSe FILMS GROWN BY REPEATED ELECTRODEPOSITION CYCLES

R. K. PANDEY*, S. R. KUMAR AND A. J. N. ROOZ

Department of Physics, Bhopal University, Bhopal 462026 (India)

S. CHANDRA

Department of Physics, Banaras Hindu University, Varanasi 221005 (India) (Received March 30, 1990; revised September 11, 1990; accepted November 29, 1990)

Photoelectrochemical studies of the n-CdSe films prepared by a repeated electrodeposition process employing *in situ* etching, cathodic deposition and annealing are reported. The influence of the anodic etching current density on the photoanodic behaviour of the films is also discussed. It is shown that better solar cell performance can be obtained by using the repeated electrodeposition process compared with the normal single-step electrodeposition. The solar cell studies have also been correlated with the experimentally determined minority carrier diffusion length and the surface morphology of the films.

1. INTRODUCTION

Cadmium selenide films electrodeposited in an aqueous acidic bath usually contain a large concentration of elemental selenium. Although a post-deposition annealing treatment removes the excess selenium, the resulting films acquire an irregular and porous surface morphology¹. These surface features tend to limit the short-circuit current, fill factor and efficiency of the CdSe-based electrochemical photovoltaic cells. In a recent report by us² it was shown that an improved crystallinity and surface morphology can be obtained by using three cycles of electrodeposition, annealing and *in situ* etching instead of the normal single cycle followed by annealing. In this paper, we shall present our results on the CdSe films prepared by repeated electrodeposition. Our findings will also be correlated with the supporting evidence obtained by scanning electron microscopy (SEM) analysis.

2. EXPERIMENTAL PROCEDURE

Cadmium selenide films were electroplated at 49 °C in an aqueous electrolyte containing AR grade $0.3 \, \text{M CdSO}_4$, $9.0 \times 10^{-4} \, \text{M SeO}_2$ and $1.5 \times 10^{-2} \, \text{M}$ ethylene diamine tetraacetic acid (EDTA). The potentiostatic deposition of CdSe on polished

^{*} Present address: Dipartimento di Chimica Fisica Applicata, Politecnico di Milano, Piazza Leonardo da Vinci 32, Milano 20133, Italy.

nickel cathode was carried out at -0.68 V referred to a saturated calomel electrode SCE.

Two sets of CdSe films were fabricated. In one set (film A) a single cycle of electrodeposition was used. The total duration of electrolysis was 10 min. These films were subsequently annealed in air at 400 °C. In the second set (film B), we employed three cycles of electrodeposition of 3.5, 3.5 and 3 min duration instead of the single deposition cycle of 10 min duration in the first set. Before the commencement of the second and third cycles, the CdSe film was first annealed in slow steps at 340 °C in air and then etched *in situ* by applying a small anodic bias to the substrate. The etching current density and the time were optimized by studying the photoanodic behaviour of the CdSe films. The final annealing after the third cycle was performed at 400 °C. Further details on the electrodeposition and annealing can be obtained elsewhere¹. The thickness of the CdSe films obtained by the two methods was approximately 1 μm.

The current-voltage characteristics of the cadmium selenide films were studied in the dark as well as under illumination from a tungsten halogen lamp. The light intensity was kept at $50 \,\mathrm{mW}\,\mathrm{cm}^{-2}$.

The biased monochromatic photocurrent response of a CdSe film-sulphide/polysulphide junction was used to determine the flat band potential, minority carrier diffusion length and donor concentration. The electrolyte used for this purpose contained AR grade 1 M NaOH, 1 M Na₂S and 1 M S. A conventional three-electrodeconfiguration was used with nickel as the counterelectrode and an SCE as the reference. The cell had a flat window for illumination of the film. Before dipping, copper lead was soldered to the nickel substrate and a common epoxy was applied to seal the metallic portions. All samples were etched in 1 N HCl for 45 s before use. A 2 mW He–Ne laser ($\lambda = 680 \, \text{nm}$) was used as a photon pump and the flux was adjusted to $1.79 \times 10^{-3} \, \text{cm}^{-3}$.

SEM was carried out with a Jeol scanning electron microscope (model JSM 35CF) at 20 kV using normal incidence.

3. RESULTS AND DISCUSSION

3.1. Solar cell studies

During the investigation of the photoanodic behaviour of the CdSe films, it was observed that the *in situ* etching before the commencement of a new electrodeposition cycle is essential for obtaining good photoactivity. Unetched films exhibited very poor photoresponses. The short-circuit current $J_{\rm sc}$, open-circuit voltage $V_{\rm oc}$, fill factor ff and efficiency η were strongly influenced by the *in situ* etching current density employed during the second and third cycles of electrodeposition. The observed dependence of these solar cell parameters on the *in situ* etching current is shown in Figs. 1 and 2. The optimized etching duration was 60·s. From these figures it is obvious that all the four parameters increased gradually and attained maximum values for an etching current density of 0.14 mA cm⁻². The *in situ* etching was expected to remove surface contaminants such as an insulating oxide layer and to provide a fresh film surface for the growth during the new electrodeposition cycle. However, the *in situ* etching at current densities greater than 0.14 mA cm⁻² was

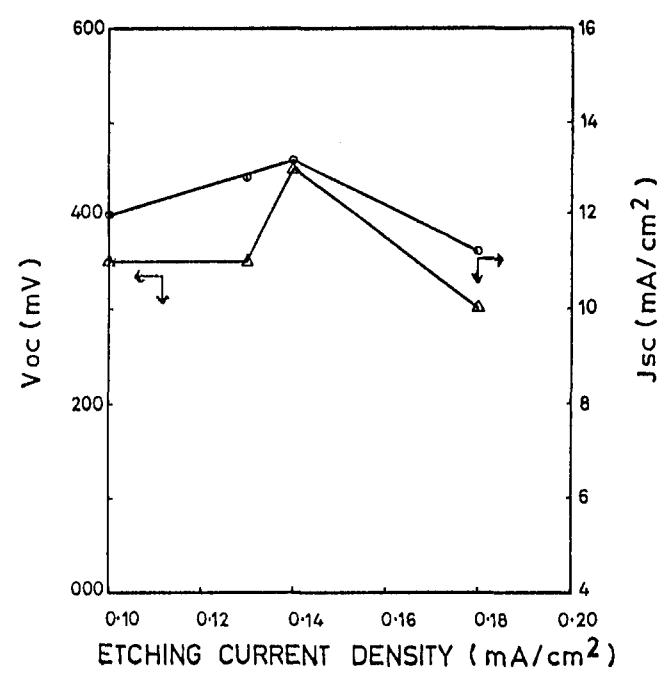


Fig. 1. Variation in the short-circuit current (\bigcirc) and open-circuit voltage (\triangle) of solar cells fabricated from CdSe films deposited using different *in situ* etching current densities.

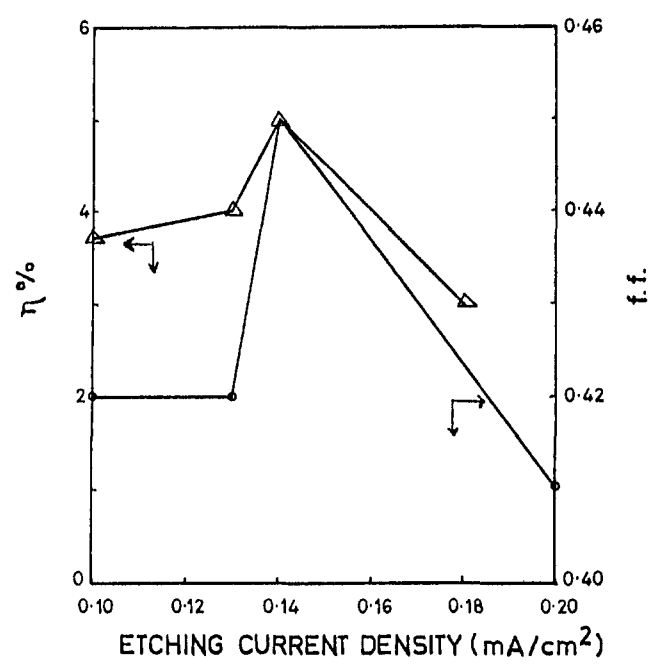


Fig. 2. Variation in the solar cell efficiency (\triangle) and fill factor (\bigcirc) with the *in situ* etching current density used for the multistep deposition of CdSe films.

often found to damage the parental CdSe film, causing pinholes and lifting. The observed decrease in the values of $V_{\rm oc}$, $J_{\rm se}$, ff and η at higher etching currents may be attributed to this surface damage.

The solar cell characteristic of a typical n-CdSe film B electrodeposited by three cycles of electrodeposition, in situ etching at $0.14 \,\mathrm{mA \, cm^{-2}}$ and annealing, is shown in Fig. 3. The performance of this film has also been compared with the annealed CdSe film A prepared by a single-step deposition. While the open-circuit voltage in both cases did not change, the short-circuit current increased from $8 \,\mathrm{mA \, cm^{-2}}$ to $13 \,\mathrm{mA \, cm^{-2}}$, the fill factor improved from 0.38 to 0.45 and the efficiency from 3.5% to 5%. The reasons for the observed improvements in the photoanodic behaviour will be discussed in the following sections.

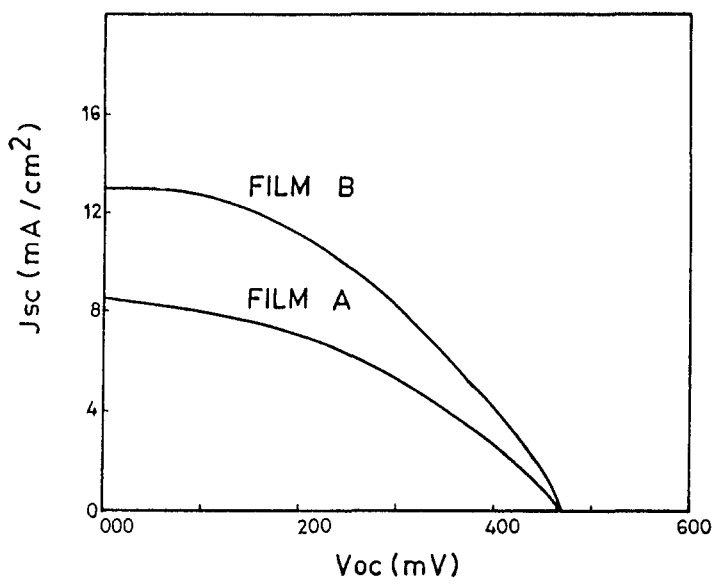


Fig. 3. Output characteristics of solar cells employing CdSe films grown using single-step (film A) and multistep (film B) electrodeposition techniques.

3.2. Dark J-V characteristics

If it is assumed that the n-CdSe film electrolyte junction behaves as a Schottky barrier, the dark J-V characteristics can be mathematically expressed as

$$J_{\mathrm{D}} = J_{\mathrm{0}} \left\{ \exp(eV/\beta kT) - 1 \right\} \tag{1}$$

where $J_{\rm D}$ is the reverse saturation current and β the ideality factor.

The dark J-V characteristics of the semiconductor-liquid junctions formed using the films A and B shown in Fig. 4 resemble the behaviour of a Schottky diode. Figures 5 and 6 show the plots of the logarithmic dark current vs. applied bias for films A and B respectively. From the slopes of the straight line plots, the ideality factors were calculated and found to be 1.54 and 1.16 for films A and B respectively. The lower ideality factor for film B implies a reduction in the forward leakage current and depletion layer recombination³.

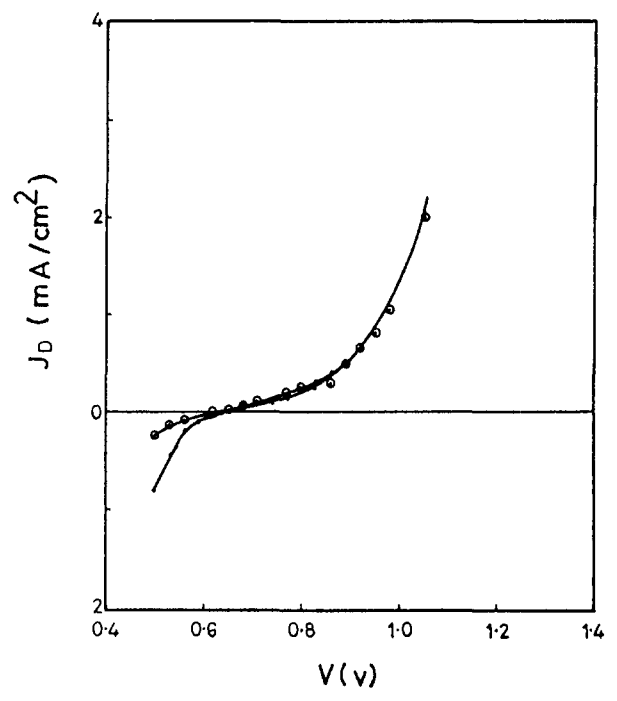


Fig. 4. Dark J-V characteristics of CdSe films deposited by single-step (\bullet) and multistep (\bigcirc) electrodeposition.

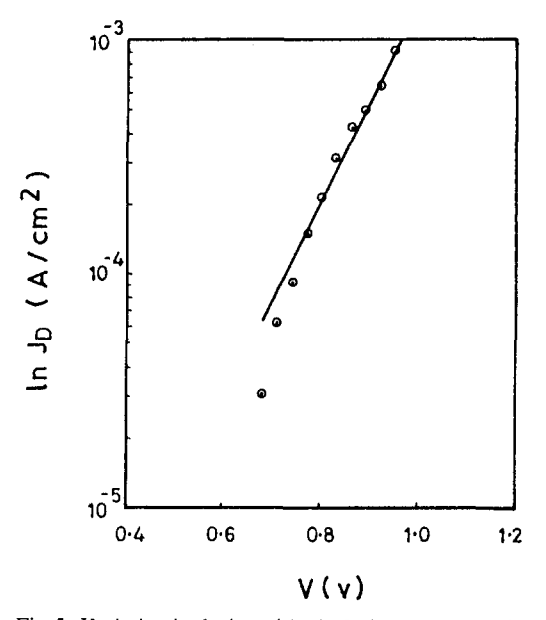


Fig. 5. Variation in the logarithmic dark current vs. voltage for a CdSe film deposited by the single-step technique.

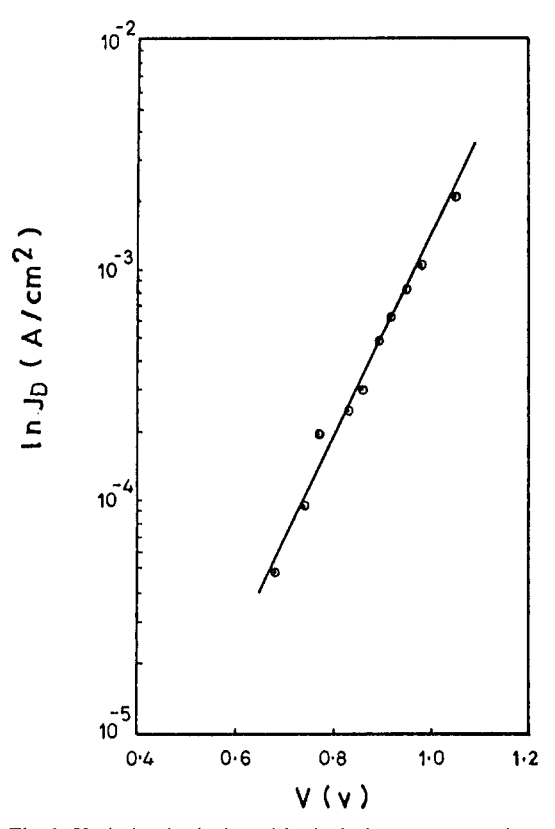


Fig. 6. Variation in the logarithmic dark current vs. voltage for a CdSe film deposited by the multistep technique.

3.3. Biased monochromatic photocurrent response

The biased monochromatic photocurrent response of the semiconductor—liquid junction has been widely used^{4–10} to obtain information on the flat band potential $V_{\rm fb}$, minority carrier diffusion length $L_{\rm p}$ and donor concentration $N_{\rm D}$. The technique is based on Butler's model⁷ which treats the semiconductor—liquid junction as an ideal Schottky barrier. The reaction kinetics and the carrier recombinations within the depletion layer as well as at the surface are ignored. The monochromatic efficiency can be expressed as

$$\eta = 1 - \exp\left[1 - \frac{\exp\left\{-\alpha(2\varepsilon\varepsilon_0/eN_D)^{1/2} (V - V_{\rm fb})^{1/2}\right\}}{1 + \alpha L_{\rm p}}\right]$$
(2)

where ε is the dielectric constant and α the absorption coefficient of the semiconductor and ε_0 is the permittivity of free space.

The linear plot of $\ln(1-\eta)$ vs. $(V-V_{\rm fb})^{1/2}$ can thus be used to calculate the donor concentration and the minority carrier diffusion length, provided that one works under sufficiently high reverse bias conditions. Figures 7 and 8 show the variation in $\ln(1-\eta)$ vs. $(V-V_{\rm fb})^{1/2}$ for films A and B respectively. Using $\alpha=3\times10^4$ (ref. 11), we obtained $N_{\rm D}$ equal to 4×10^{15} cm⁻³ and 1.8×10^{15} cm⁻³ and $L_{\rm p}$ equal to 0.31 μ m

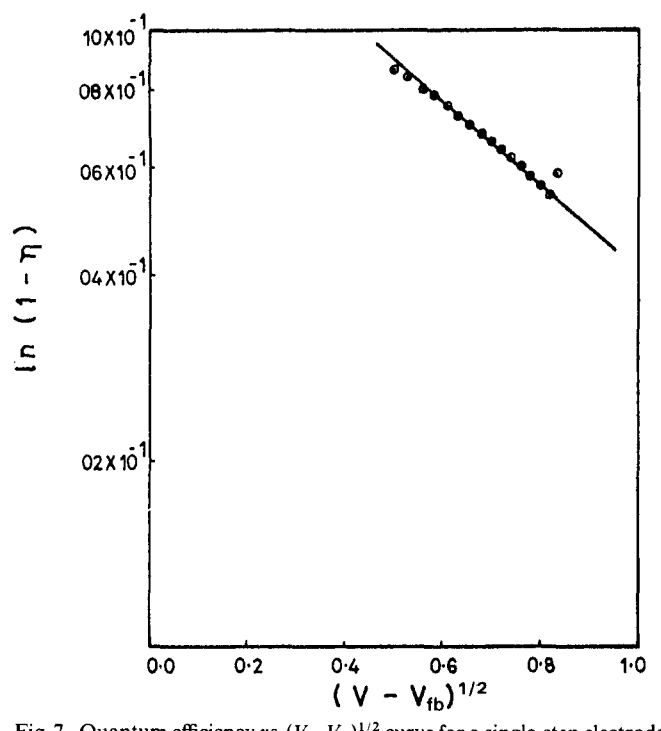


Fig. 7. Quantum efficiency vs. $(V-V_{\rm fb})^{1/2}$ curve for a single-step electrodeposited CdSe film.

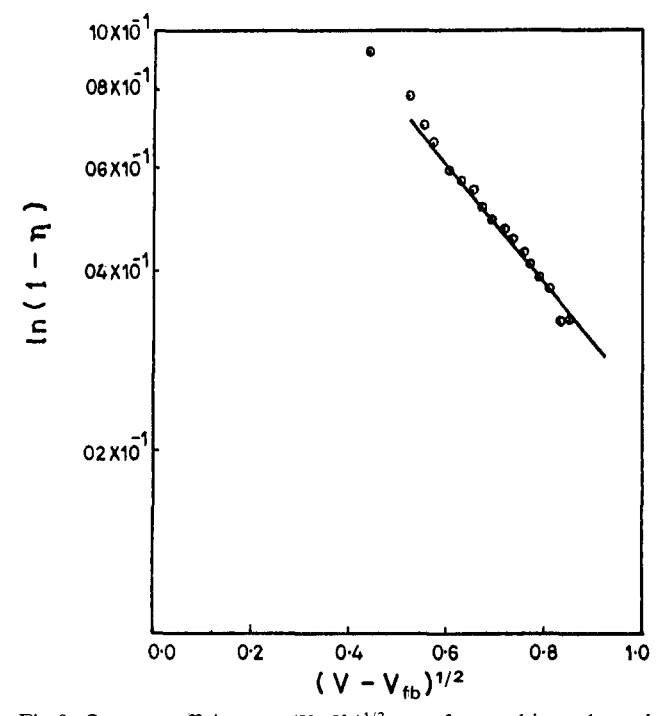
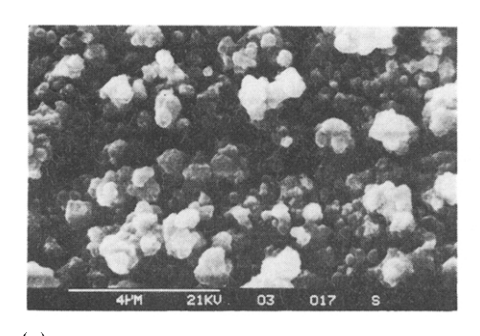


Fig. 8. Quantum efficiency vs. $(V-V_{\rm fb})^{1/2}$ curve for a multistep electrodeposited CdSe film.

and 0.47 μ m respectively for films A and B. Evidently, the three cycles of electrodeposition result in an approximately 50% higher value of the minority carrier diffusion length in film B. In polycrystalline materials, the minority carrier diffusion length is mainly limited by grain boundary recombination. The higher value of L_p in film B can be attributed to a reduction in the grain boundary recombination due to the increased grain size. This conclusion has been further vindicated by the SEM analysis of the CdSe films.

3.4. Surface morphology studies

Figure 9 shows the surface morphologies of annealed films A and B as revealed by SEM. The difference in contrast between the surface particles (lighter contrast) and the bulk (darker contrast) in film A indicates a porous surface. The grains are also not in good electrical contact with each other. On the contrary, an improved surface morphology with considerably reduced charging effects can be seen in Fig. 9(b) for film B. The average grain size in this case is also larger (0.75 μm as against 0.47 μm in film A). Detailed structural characterization of the films using X-ray diffraction was also carried out by us and the results support this conclusion¹².



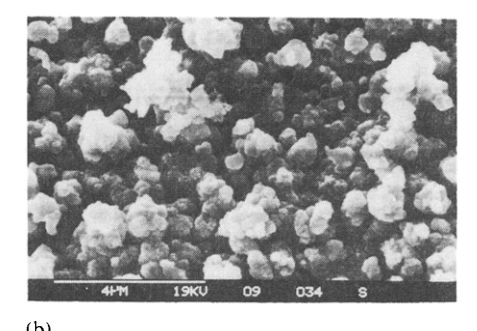


Fig. 9. Surface topology of (a) the single-step deposited and annealed and (b) the multistep deposited and annealed CdSe films.

Our studies thus clearly highlight the benefits accrued from the multistep deposition of CdSe films. The purpose of annealing after every deposition cycle was to remove the excess selenium which would otherwise passivate the surface. The selenium excess is also likely to impart an insulating character to the electrode surface, particularly when the deposition proceeds for longer durations. For thicker films, therefore, the discharging constituents, after some time, may not adhere well, giving rise to a porous surface morphology such as in film A. In fact, in all the CdSe films deposited by single-step deposition, a poorly adhering upper layer was always observed over an inner compact and strongly adhering deposit. The repeated cycles of electrodeposition also cover the micropores normally present in the electrodeposited semiconductor films. These microscopic pinholes provide shunting paths for the photogenerated carriers, resulting in a high forward leakage current. The dark J-V characteristics also yielded a higher value of the ideality factor in film A, indicating a defective surface morphology. One may also, therefore, correlate the observed lower values of the short-circuit current in the case of film A with the

presence of pinholes, which increase the leakage current. Another beneficial aspect of the multistep deposition is that the grains of the parental layer provide fresh nucleation sites for subsequent growth during a new cycle of deposition. This results in a better surface morphology with higher grain size. The overall effect is manifested in the increase in the minority carrier diffusion length and reduced forward leakage current, and hence increased short-circuit current, efficiency and fill factor of solar cells.

4. CONCLUSIONS

Our studies indicate that a repeated electrodeposition process should be preferred over a normal single-step deposition for a longer duration. A considerably improved photoanodic behaviour was observed in the case of films electrodeposited by the multistep process incorporating in situ etching and annealing. The short-circuit current increased from 8 mA cm $^{-2}$ to 13 mA cm $^{-2}$ and the minority carrier diffusion length increased from 0.31 μm to 0.47 μm . The solar cell efficiency and fill factor also registered improvements. The SEM examination of the films revealed a more regular surface with increased grain size in the case of films deposited by three cycles of electrodeposition. It would be interesting to extend this technique to the electrodeposition of other compound semiconductors.

ACKNOWLEDGMENT

This work was supported by the research grants received from the Department of Nonconventional Energy Sources, New Delhi, which is gratefully acknowledged.

REFERENCES

- 1 R. K. Pandey, A. J. N. Rooz and S. K. Kulkarni, Thin Solid Films, 150 (1987) 57.
- 2 S. R. Kumar, R. K. Pandey and A. J. N. Rooz, Bull. Electrochem., 5 (1989) 711.
- 3 H. J. Hovel, in A. Beer and R. Willardson (eds.), Semiconductors and Semimetals, Vol. 11, Solar Cells, Academic Press, New York, 1975, p. 124.
- 4 R. K. Pandey, R. B. Gore and A. J. N. Rooz, J. Phys. D, 20 (1987) 1059.
- 5 M. Cadorna, K. L. Shaklee and F. H. Pollak, Phys. Rev., 154 (1967) 696.
- 6 R. H. Sprunken, R. Schumacher and R. N. Schindler, Faraday Discuss. Chem. Soc., 70 (1980) 55.
- 7 M. A. Butler, J. Appl. Phys, 48 (1977) 1914.
- 8 J. Gautron and P. Lemasson, J. Cryst: Growth, 59 (1982) 332.
- 9 W. W. Gartner, Phys. Rev., 116 (1959) 84.
- M. A. Russak, J. Reichman, H. Witzke, S. K. Deb and S. N. Chen, J. Electrochem. Soc., 127 (1980)
- 11 S. M. Sze, *Physics of Semiconductor Devices*, Wiley Eastern, New Delhi, 1979, p.21.
- 12 R. K. Pandey, S. R. Kumar, A. J. N. Rooz and S. Chandra, J. Mater. Sci., (1991), to be published.